Published in final edited form as:
Ann Biomed Eng. 2011 November ; 39(11): 2823–2834. doi:10.1007/s10439-011-0362-x.

In Vivo Contrast-Enhanced MR Imaging of Direct Infusion into Rat Peripheral Nerves

Xiaoming Chen[1,†], **Garrett W. Astary**[2], **Thomas H. Mareci**[3], and **Malisa Sarntinoranont**[1,*]
[1]Department of Mechanical and Aerospace Engineering, University of Florida, Gainesville, FL
[2]Department of Biomedical Engineering, University of Florida, Gainesville, FL
[3]Department of Biochemistry and Molecular Biology, University of Florida, Gainesville, FL

Abstract

Direct infusion, or convection-enhanced delivery (CED), into peripheral nerves may provide a method for delivering substances to the intrathecal space or specific fiber bundles entering the spinal cord. To better understand this potential delivery technique, we have characterized the extracellular transport of macromolecular agents from peripheral nerves to the spinal cord in magnetic resonance (MR) imaging studies. High-resolution dynamic contrast-enhanced MR imaging at 11.1 T was used to monitor and characterize *in vivo* the extracellular transport dynamics of Gd-DTPA-albumin tracer during CED into rat sciatic nerves. Extracellular tracers followed peripheral nerves towards the spinal cord and at vertebral levels L4 and L5 appeared to enter the cerebrospinal fluid and nerve roots. Uptake directly into spinal cord tissues (white and gray matter) appeared to be limited. Spatial distribution patterns within spinal cord regions depended on CED factors, including cannula placement, and underlying tissue structures including peripheral nerve branching and membrane structures at nerve root entry. The applied MR techniques allowed for visualization and quantification of tracer spread and distribution within the rat spinal cord region. The results show that CED into peripheral nerves provides an alternative route for delivering therapeutics to nerve roots and the intrathecal space surrounding the spinal cord.

Keywords

albumin-Gd-DTPA; convection-enhanced delivery; DCE-MRI; nerve root

INTRODUCTION

Convection-enhanced delivery (CED) into tissues of the central nervous system (CNS) bypasses the blood-brain-barrier and directly delivers macromolecular therapeutic agents into the extracellular space. CED relies on enhanced extracellular transport and significantly increases volumetric spread into tissue. CED has proven to be a promising targeted drug delivery method for neurodegenerative diseases and injury [4, 11–13]. Most studies have focused on CED into the brain and spinal cord [4, 11–13, 22]. Few studies have focused on infusions into peripheral nerves [14, 17], and only a single study investigated transport from peripheral nerves to the spinal cord [17]. Delivery of therapeutics along peripheral nerves to the spinal cord may provide a route to treat peripheral nerve injury and administer agents to

[*]**Correspondence to:** Dr. Malisa Sarntinoranont, Department of Mechanical and Aerospace Engineering, 212 MAE-A, University of Florida, Gainesville, FL 32611, msarnt@ufl.edu, Tel: (352) 392-8404, Fax: (352) 392-7303.
[†]Now at Fox Chase Cancer Center, Philadelphia, PA

the spinal cord for chronic pain. Compared to intrathecal injection, CED into peripheral nerves may provide a delivery method for targeting specific nerve fiber bundles confined by the epineurium, entering the spinal cord and overcomes diffusion limited transport associated with intrathecal injection.

Transport of compounds within the peripheral and central nervous system is influenced by the anatomy and the underlying microstructure. As background information, Figure 1A illustrates the anatomical structure in the spinal cord region. The spinal cord is enclosed by meninges which are made up of an innermost pia mater, an arachnoid mater and an outmost dura mater. Between the pia mater and arachnoid mater is the intrathecal (subarachnoid) space which is filled with cerebrospinal fluid (CSF). Connecting to the dura mater are numerous external spinal nerves (peripheral nerves). These nerves enter the CSF by crossing the dura mater and arachnoid mater and divide into two internal dorsal and ventral nerve roots which span the intrathecal space and connect to the spinal cord. For simplicity, the region within the vertebral foramen invested by the dura mater is referred to as the spinal cord region and is comprised of the spinal cord, spinal nerve roots and CSF. The external anatomy of the rat sciatic nerve, spinal cord, and connected spinal nerves is shown in Fig. 1B. The sciatic nerve divides into two major branches, spinal nerves L4 and L5, which enter the dura mater at different sites. There is also a small nerve connection between spinal nerves L4 and L3. Also, spinal nerves L4 and L5 have long internal nerve roots (~4 cm) spanning the intrathecal space. CED and monitoring of tracer transport into the peripheral nerve and spinal cord region may also provide useful information about the communication pathway between these structures.

A couple of studies of CED into peripheral nerves have been conducted previously by Lonser et al. and Ratliff and Oldfield [14, 17]. Lonser et al.[14] examined the use of CED to deliver and distribute macromolecules into peripheral nerves of primates. Ratliff and Oldfield[17] assessed the capacity of CED to carry macromolecules across sites of peripheral nerve injury in rat and primate models and examined the functional effects of CED on intact nerves. These studies showed macromolecular protein tracers (Gd- and radio-labeled albumin) to be well-contained by the epineurium and to fill long segments of peripheral nerves after CED. Additional experiments were also conducted by Ratliff and Oldfield[17] to investigate the possibility of delivering macromolecules over a larger distance to the spinal cord by CED into the sciatic nerve. This study was done in two primates and Gd-labeled albumin tracer was observed in spinal cord gray matter in MR images acquired after infusing a large volume of infusate (~60–85 μL)[17]. However, details about the transport route from peripheral nerves to the spinal cord are still not well understood and need further study. Experimental studies in a small animal model which take advantage of advanced MR imaging techniques and allows monitoring of the transport dynamics would be useful to better characterize the CED transport routes from the peripheral nerve to the spinal cord.

Contrast-enhanced MR imaging has been used in previous in vivo CED studies to visualize distribution patterns of MR-visible agents at the end of infusion [10, 13, 14, 17]. Fewer studies have used MR imaging to monitor transient transport during infusion. For example, Krauze et al. used consecutive MR scans to monitor changes in the CED distribution of Gd-labeled lipsomes in non-human primate brains [10]. In smaller animals such as rats, in vivo MR imaging studies of the peripheral nerve and spinal cord are scarce due to the challenges of small feature dimensions (e.g., ~4 mm rat spinal cord diameter and ~1.5 mm sciatic nerve diameter) and motion-induced artifacts (e.g. breathing) [2, 3, 8, 15]. High resolution MR imaging methods provide a means to monitor and quantify CED transport in vivo in rat spinal cord regions.

The purpose of this study was to investigate CED into rat sciatic nerves as an alternative drug delivery route to the spinal cord region by characterizing infusion transport from the peripheral nerve to the spinal cord. High-resolution dynamic contrast-enhanced MRI (DCE-MRI) at 11.1 T was used to monitor the spread and distribution of MR-visible tracers within spinal cord regions during CED. A large molecular weight extracellular tracer, Gd-DTPA-albumin, was used. Surgical CED and DCE-MRI protocols are presented, tracer distribution characteristics are reported, and parameters affecting CED transport are discussed. Results from this study may improve our understanding about agent transport dynamics and routes from peripheral nerves to the spinal cord.

MATERIALS AND METHODS

Infusion System Setup

An MR-compatible, non-compliant infusion system was designed which consisted of a gas-tight syringe (100 μL luer-tip syringe, Hamilton, Reno, NV), PEEK tubing (~8 feet), and a silica cannula (outside diameter = 108 μm, inside diameter = 41 μm) (Fig. 2). The silica infusion cannula was connected to the PEEK tubing by a gas-tight microfluidic connector. Precautions were taken so that there was no fluid leakage and air bubbles were eliminated from the infusion system. Once assembled and filled with the tracer compound, the infusion system was driven by a syringe pump remotely placed in a control room shielded from the high magnetic field.

Gd-DTPA-albumin was used as the primary infusate in this study. Gd-DTPA-albumin (10 mg/mL in PBS solution; MW ≈ 87 kDa; ~35 Gd-DTPA molecules per albumin molecule; R. Brasch Laboratory, University of California, San Francisco, CA) was used to mimic transport of a macromolecular compound. In addition, Gd-DTPA (2 mg/mL in phosphate buffered saline (PBS) solution; MW = 573 Da; Omniscan, GE Healthcare, Princeton, NJ) was used in preliminary scans for protocol development. To detect the tracer distribution, the infusate concentration should be properly selected since a high tracer concentration can weaken the MR signal due to the transverse relaxation (T_2) effects and distort the distribution pattern. Also, concentrations that are too low may be undetectable due to limitations of the signal-to-noise ratio in the MR measurement [7]. To ensure proper enhancement, tracer infusate concentrations were optimized in a pilot MR imaging study where different concentrations of Gd-bound tracer were infused into CNS tissues. In addition, tracer solutions were mixed with Evans blue dye (MW = 960 Da) for post-mortem visualization. Evans blue does not bind to Gd-DTPA but binds to Gd-DTPA-albumin. For the latter tracer, the concentration of Evans blue (1.8 mg Evans blue per 5 mL solution of Gd-DTPA-albumin) was low enough to ensure it was completely bound to albumin and avoid any unbound Evans blue[18], which would be inappropriately identified as Gd-DTPA-albumin tracer during post-mortem investigation.

Animal Preparation

Rat studies were conducted in accordance to a protocol reviewed and approved by the Institutional Animal Care and Use Committee of the University of Florida and included four adult female Sprague-Dawley rats weighting 250–270 g (experimental data from an additional four rats were obtained in protocol development studies). Rats were initially anesthetized using 4% isoflurane, and maintained under anesthesia (1.5–2% isoflurane) during surgery and MR imaging. Throughout the course of MR imaging, rat respiration was monitored using a respiratory sensor pillow and heated airflow was supplied to keep the animal warm.

For CED surgical preparation, the sciatic nerve in the right lower extremity was exposed for cannula insertion by incising the skin and retracting the gluteus muscles (Figs. 2A–B). The incision was extended proximally to the sciatic notch where the silica infusion cannula was inserted into the sciatic nerve (diameter ~1.5 mm) and directed cranially into the intrapelvic portion of the nerve to an insertion depth of 3.5 to 4 cm. The cannula insertion point in the sciatic nerve was ~5 cm distal to the L5 nerve-dura mater junction. Preliminary CED studies using Gd-DTPA were conducted for a shorter cannula insertion depth of ~1 cm (Fig. 4). Gd-DTPA was found to be well contained by the epineurium with no visible tracer outside of the peripheral nerve. Tracer distributed within the sciatic nerve (arrow 1), as well as into spinal nerves L4 (arrows 2, 4 and 6) and L5 (arrows 3, 5 and 7). However, a limited amount of Gd-DTPA tracer entered the spinal cord region (arrow 7) even after a large infusion volume was introduced. This result prompted a change in the cannula insertion depth closer to the spinal nerve-dura mater junction. CED transport of Gd-DTPA to the spinal cord region was confirmed in an additional rat. Next, the infusion cannula was secured and sealed in the nerve by tissue adhesive (Vetbond, 3M, St. Paul, MN). The surgical wound was closed using monofilament sutures with a small opening left for the cannula to exit. Before the start of infusion, the rat remained anesthetized an additional ~60 min. During this period, MR imaging setup was conducted, which included tuning of RF coil circuits, positioning the rat in the magnet system, and acquiring pre-infusion scans.

In vivo experiments required simultaneous animal care, CED surgery and infusion into small peripheral nerves, and tuning of coupled RF coils. Four rats underwent peripheral nerve CED with Gd-DTPA-albumin using an infusion rate of 0.3 μL/min (12–47 μL). Since the maximum field of view (FOV) of the surface coil was limited to approximately 5 cm along the length of the spinal cord (the axial geometric length of the surface coil is ~3 cm), infusate volumes were restricted to < 50 μL (less than ~15% of total intrathecal CSF volume in adult rats, which is 300 to 400 μL [20]) so that tracer distributions were well contained in the MR FOV. Following CED and MR imaging procedures, rats were sacrificed immediately, and post-mortem surgery was conducted to examine the tracer distribution and cannula position.

MR Imaging

MR imaging measurements were performed on a Bruker Avance Console (Bruker NMR Instruments, Billerica, MA) with a Magnex Scientific magnet system (11.1 Tesla / 40 cm horizontal bore; Magnex Scientific, Oxford, UK). The imaging apparatus included a custom radio-frequency (RF) dual coil system with a large volume coil for excitation and a small surface coil for detection (Fig. 2C).

For DCE-MRI, multi-slice T_1-weighted images were acquired using a spin echo sequence with a fat suppression. Alternative sagittal and transverse scans were used to obtain a complete picture of the infused region. The following imaging parameters were used during CED: for transverse scans, TR = 330 ms, TE = 8 ms, average = 5, FOV = 2 cm × 2 cm, image matrix = 96 × 96, number of slices = 10; for sagittal scans, TR = 330 ms, TE = 8 ms, average = 4, FOV = 2 cm × 4 cm, image matrix = 96 × 192, number of slices = 10. The resulting image resolution was 0.2 mm × 0.2 mm × 1 mm per voxel, and the resulting scan times were 2 min 38 sec for each transverse scan and 4 min 13 sec for each sagittal scan. MR data sets were acquired consecutively, and each data set included two transverse scans and one sagittal scan. The time interval between each data set was ~10 min. For all scans, an anatomical region roughly from vertebral levels L6 to L1 was covered. Two pre-infusion MR scans were conducted which were used as references of the pre-contrast enhanced signal so that the tracer distribution region in the MR scans during CED could be identified. Following that, MR scans and infusion of Gd-DTPA or Gd-DTPA-albumin started simultaneously and MR scans were repeated consecutively until the infusion was complete.

In addition, before and after CED, transverse MR scans at a higher resolution were also obtained to better distinguish tracer distributions in various tissue regions (TR = 1000 ms, TE = 10 ms, FOV = 2 cm × 2 cm, image matrix = 128 × 128, average = 3).

MRI Data Processing

Raw MRI data was processed using custom software written in the Interactive Data Language (Research Systems, Inc., Boulder, CO) and resolution was interpolated bilinearly by a factor of 2. The distribution volume (Vd) of the tracer in the spinal cord region was estimated from these images using a MATLAB routine (version 6.5, The MathWorks Inc., Natick, MA) in which tracer-filled regions were contoured by comparing the signal intensity of tracer-filled voxels with those without tracer. Final contours of tracer-filled regions were confirmed by visualizing the contours on MR images. Only voxels in the CSF, nerve roots, and spinal cord tissues were counted, and the tracer-filled voxels in peripheral nerves were excluded in Vd. The total tracer distribution volume was calculated by adding together the voxel volumes in each transverse MR scan. Within the tracer-filled region, percent signal enhancement (PSE) was also calculated which defined as the percentage of the MR signal change before and after infusion. Within the spinal cord region, nerve root distributions were defined in transverse images as distinct bright spots that did not expand with time. In addition, the axial length of the tracer-filled region in the spinal cord region was estimated from sagittal scans.

RESULTS

A typical MR scan of the rat spinal cord region with fat suppression is shown in Fig. 3. The anatomical structure including gray matter (GM) and white matter (WM) can be clearly identified at high vertebral levels, but cannot be seen at low vertebral levels due to the small cross-sectional diameter of the spinal cord at vertebral levels L4 to L6. At these levels, the spinal cord is mainly filled with cranial-caudally aligned nerve roots which originate from lower vertebral levels. Preliminary CED studies using Gd-DTPA tracer included a FOV with greater coverage of the peripheral nerves. For sciatic nerve CED, these scans clearly showed that the extracellular tracer tracked along external nerve pathways before entering the spinal cord region via spinal nerves L4 and/or L5 (Fig. 4). Also, tracers were found to be well contained by the epineurium with no visible tracer outside of the peripheral nerve. Postmortem analysis showed that Evans blue tracer distributions in the vicinity of the infusion cannula were mainly on the side directed towards the spinal cord, indicating that tracer moved primarily in the direction of the spinal cord from the point of infusion. Evans blue tracer distribution in peripheral nerve branches was also observed, e.g., in the thin nerve connection between L4 and L3 nerves.

Gd-DTPA-albumin tracer spread within the spinal cord region was imaged in sagittal and transverse MR scans (Fig. 5) and consistent CSF and nerve root uptake was observed. CSF distributions were delineated by large transverse tracer spreads (arrow 6) and by distributions confined along the edges of the spinal cavity or dura mater (arrows 1 and 9). CSF distributions were verified by comparing the PSE in proposed CSF regions to PSE calculated in nerve roots containing tracers. PSE values in the regions proposed to be nerve roots were found to be four to ten times higher than values calculated in the delineated CSF regions, and tracer concentrations in the CSF were more diluted than in the proposed nerve root regions. Nerve root distributions were identified in transverse images as distinct bright spots that did not expand with time (Fig. 5 arrow 2; Fig. 6 arrows 3 and 8). Post-mortem tissue analysis validated spinal nerve root uptake with Evans blue tracer visible in both dorsal and ventral nerve roots. CSF distribution patterns were found to differ between animals, varying between large transverse and cranial-caudal tracer spread (arrow 6 in Fig. 5) to more peripheral distributions (arrows 9 and 10 in Fig. 5). However, for all rats tracers

were confined within the dura mater and moved primarily in the cranial direction with increasing infusion volumes, as can be seen in the sagittal scans in Fig. 5 and also in consecutive sagittal scans in Fig. 6.

Gd-DTPA-albumin tracer transport dynamics were captured through consecutive MR scans, as shown in Fig. 6. MR scans showed tracer first entering the spinal cord region through the L4 spinal nerve at the vertebral level L4 after approximately 12 μL of the tracer infusion (arrows 1 and 2). Tracer spread primarily in the cranial direction upon entry. Nerve root distribution was first observed after ~15 μL at vertebral level L4 (arrow 3). Tracer leakage from the nerve root was not evident since the enhanced spot did not enlarge with time (15–30 μL) in transverse scans. With continued infusion (~30 μL), a tail-like expansion from the enhanced nerve root around the spinal cord was observed (arrow 7). This expansion may be due to tracer tracking upwards within the CSF surrounding the nerve root as observed in sagittal scans (22–47 μL, arrows 4, 6 and 9). At this later infusion time, tracer also entered the spinal cord region through the L5 nerve at vertebral level L5 (arrow 5), and nerve root uptake of tracer at vertebral level L3 was also evident (arrow 8). Nerve root distributions increased with the tracer infusion volume and covered a large cranial-caudal distance from vertebral levels L4 to L3 for infusions greater than 30 μL (arrow 10).

Total Gd-DTPA-albumin infusion volumes (Vi) and distribution volumes (Vd) in the spinal cord region are compared in Fig. 7. It should be noted that Vi is the total volume infused at different time points. Vd is the distribution volume in the spinal cord region (including CSF, nerve root, and spinal cord tissue) not including tracer distribution in the peripheral nerve. In this graph, a typical curve includes an initial flat region (i.e., time lag) followed by a rapid increase in distribution volume with infusion time. The duration of the time lag corresponds to 3–10 μL of infusate as estimated from the graph. In other words, it took approximately 10–33 min for the tracer to reach the spinal cord region. Following this time lag, Vd increased with increasing Vi. In most of these experiments, ratios of Vd and Vi increments were approximately consistent (slope = 1.67±0.32). For one experiment, slow uptake was also reported (slope = ~0.4). For this animal, post-mortem analysis determined the cannula tip to be at a shorter insertion depth (in the L4 nerve near the L4-L5 nerve bifurcation) which resulted in significant infusate diversion into the L5 nerve.

In post-mortem analysis, cannula tip locations and insertion depths were measured (Table 1). No tip penetration or tissue tearing across the sciatic nerve epineurium was observed in any rat. However, in all rats some Evans blue tracer stains were observed in the tissue surrounding the sciatic nerve in the vicinity of the cannula tip, i.e., staining adjacent muscle tissue. This leakage was not observed directly in MR scans since the cannula tip was outside of the imaging FOV. In one instance, MR signal enhancement in regions outside of nervous tissues was observed along the outside boundary of the vertebral bone (arrows 7 and 8 in Fig. 5) which may indicate the tracer leaked out of the sciatic nerve near the cannula tip and spread in the surrounding tissue. Post-mortem Evans blue distributions showed qualitative consistency with Gd-DTPA-albumin distributions on MR images, such as the distribution of both tracers in CSF and nerve roots. In CSF, observed Evans blue color was diluted while it was much darker in nerve roots (both dorsal and ventral nerve roots). Quantitative comparison of Evans blue distribution volumes with MRI results is difficult (involving post-mortem tissue slicing, image registration and segmentation) and was not conducted.

DISCUSSION

Previous studies of peripheral nerve infusion showed tracer transport within peripheral nerves[14, 17] and Ratliff et al. [17] also showed tracer distributions in the spinal cord gray matter after peripheral nerve retrograde infusion in primates. As an extension of those

studies, this study further investigated dynamic aspects of peripheral nerve CED transport *in vivo* and the potential for peripheral nerve CED as a new drug delivery method for the spinal cord region by using a small animal model combined with advanced high-resolution MR imaging. By using DCE-MRI, extracellular transport routes from peripheral nerves to the spinal cord region were studied and experimental results showed spinal cord tracer distributions to be well characterized and certain tracer transport patterns were observed: 1) Within the peripheral nerve, tracers were well-confined by the epineurium with tracer moving primarily in the direction of the spinal cord. 2) Consistent CSF and nerve root uptake was observed with little uptake in spinal cord tissue and tracer entry into CSF and nerve root occurred immediately following its exit from peripheral nerves. 3) Within the intrathecal space, tracers were well-confined by the dura mater and moved primarily in the cranial direction. 4) There was an accumulation of spinal tracers with increasing infusion volumes and tracer distributions were approximately proportional to the volume infused. Overall, while no tracer was observed to reach the spinal cord tissue, significant tracer quantities were found to reach the spinal cord region (CSF and nerve roots) with careful placement of the infusion cannula. Thus for the rat animal model, CED into peripheral nerves was shown to provide a potentially new way to deliver drugs into the intrathecal space and to nerve roots adjacent to the spinal cord.

Notably, CSF uptake of tracer compounds was clearly observed in this study. This finding is consistent with a previous tracer distribution study by Pettersson that looked at tracer transport in the opposite direction, from the CSF to the nerves [16]. In his study, Evans blue-albumin tracer was injected intrathecally into the CSF of a rat. Both macroscopic and microscopic examinations of tissue samples showed tracer distribution in the spinal nerve roots and peripheral nerve indicating that a communicating pathway exists from CSF to nerve roots and peripheral nerves. However it was not clear how the tracer entered these structures from CSF. In our *in vivo* real-time imaging study, early tracer distributions in CSF appeared near nerve root entry into the subarachnoid space indicating early leakage at the junction between the dorsal and ventral roots or across nerve root sheaths. This supports the idea that there is likely a communicating pathway between peripheral nerve and CSF at the junction between dorsal and ventral roots as suggested by Himango and Low [9]. Their structural analysis studies showed peripheral extensions of the subarachnoid space, i.e., lateral recesses, between dorsal and ventral roots that were filled with cellular debris and macrophages. They suggested that this region is likely a communicating pathway between peripheral nerves and the CSF.

Several factors influenced extracellular tracer transport from the peripheral nerve to the spinal cord region. Extracellular and fluid transport of Gd-DTPA-albumin was considered to be by convection and diffusion transport mechanisms. Transport analysis of a tracer confined within a nerve root in the spinal cord region reveals a Peclet number on the order of 100 indicating convection-dominated delivery within this region [Peclet number is defined as Pe = LV/D, where L is the characteristic length scale of the nerve root diameter (~1 mm), V is the tracer transport velocity (~10^{-4} cm/s in the nerve root calculated using DCE-MR images), and D is the tracer diffusivity in the nervous tissue (~ 10^{-7} cm^2/s) [19]]. This convection-dominated transport enhanced tracer delivery in the spinal cord region. The maximum tracer transport distance during CED may be constrained by several factors. For example, a typical nerve root length from the L5 nerve-dura mater junction to the nerve root entry into the spinal cord was approximately 4 cm. For tracer distributions to cover this long travel distance large infusion volumes were required, but infusate could also flow into other regions such as the CSF and other nerve branches of the sciatic nerve, e.g., the thin connection between L4 and L3. Infusion into such a system with multiple sinks increases the infusion volumes required for tracer or drugs to reach the spinal cord. As a result, the majority of tracer was observed to distribute within the CSF due to leakage at junctions and

across membranes. As an additional consideration, the fluid resistance of the CSF system (total CSF volume in adult rats is 300 to 400 μL [20]) may also increase with continued infusion and hinder transport into the intrathecal space. In addition, tracers were found to enter spinal cord regions through either the L4 or L5 nerves. This is consistent with the fact that sciatic nerve branches into L4 and L5 nerves before entering the spinal cord region. Dominant pathways appeared to be related to the location of the cannula tip, e.g., infusion sites closer to or in the L4 nerve resulted in more tracers being transported through this nerve. These patterns may also be affected by anatomical factors such as pathway variation within nerve bundles between animals [1].

Within the intrathecal space, variable tracer distribution patterns were observed in CSF. This was as expected since there are likely differences in tissue structure within this space, e.g., nerve root positions and the oscillatory fluid flow patterns which are sensitive to these structures will vary between animals. Overall, CSF distributions were confined by dura mater. Bulk fluid movement of tracers in the cranial direction may have been due to the angle of entry of the spinal nerves at the spinal nerve-dura mater junction or due to less intrathecal fluid resistance in the cranial direction.

Additional transport routes were also observed. Some localized tracer leakage was noted across the epineurium in the vicinity of the cannula tip. Although the epineurium is generally poorly permeable to the tracer, these instances of tracer membrane penetration may have been due to locally high infusion pressures that change the structure to allow tracer leakage, e.g., increased pore size. These pressures would decrease with distance from the infusion site. Lower infusion rates would reduce this effect.

The plot of the distribution volume in the spinal cord region (Vd) against the infusion volume (Vi) showed an initial flat region. The flat section corresponds to the time lag before the tracer entered the spinal cord region and during this period, tracer transported only in the peripheral nerve, which was not included in Vd as defined in this study. The duration of this lag likely depends on the distance with the sciatic nerve traveled, i.e., from the cannula tip location to the spinal cord region. In most of these experiments, the trend of increasing Vd with increasing Vi was consistent once tracer entered the spinal cord region. The experiment with slower uptake was due to a relatively shorter insertion depth and diversion of infusate through the peripheral nerve network which resulted in less infusate reaching the spinal cord region. In addition, tracer distribution in the spinal cord region may be affected by other CED parameters such as infusion rate and diameter of the infusion cannula. Such factors have been investigated by Chen et al.[6] for CED in the rat brain and such a sensitivity analysis was not the focus of this study. However, particularly for this study, one of the important factors that affect CED and tracer transport to the spinal cord is location of the cannula tip within the peripheral nerve.

In this study, an RF dual coil system, consisting of a bird-cage volume coil for excitation and a quadrature surface coil for reception, was used for MR imaging. The large volume coil can achieve a higher RF field uniformity during excitation while the surface coil provides enhanced sensitivity during RF reception [5]. A system combining these two characteristics can achieve a good sensitivity and a relatively large FOV. This is particularly useful for rat spinal cord and peripheral nerve imaging due to the high resolution required to capture small features. Even at the high MR resolution used in this study, images did not provide fine structural details of small transverse nerve roots, and there was low signal contrast between CSF and these nerve roots. This constraint limited quantification in the CSF and finer nerve root structures.

Simultaneous imaging and delivery of compound agents via sciatic nerve CED into the spinal cord is technically challenging. The low infusion rate used in this study together with the surgery and experiment setup required a long experiment time in order to deliver enough volume of infusate, which increased the difficulty on animal care. These factors made it difficult to perform a large number of experiments. However, the main purpose of this study was to monitor tracer transport from peripheral nerves to the spinal cord. This extracellular transport phenomenon was considered a stable physical process, i.e., macromolecular transport in a confined media, similar to a tube, which is composed of fluid and solid fibers with no significant chemical or biological reactions.

The MRI techniques used in this study successfully monitored transport dynamics in rat spinal cord regions *in vivo* and the developed techniques are useful for future spinal cord transport studies. Tracer transport pathways from peripheral nerves to the spinal cord region were illustrated *in vivo* and CED into peripheral nerve was shown to provide a potentially new way to deliver drugs into the intrathecal space and to nerve roots adjacent to the spinal cord. In this study, the sciatic nerve was chosen due to its accessibility. However, the long distances required for infusate transport and diversion of tracers to the intrathecal space appear to be obstacles for delivery directly to spinal cord tissues. CED into other peripheral nerves that have shorter nerve roots may achieve the drug delivery into the spinal cord tissue. In addition, even though previous studies show that CED into brain tissue is safe [4, 13], inserting a cannula into the sciatic nerve may cause peripheral nerve damage. To evaluate the potential clinical application of this peripheral nerve CED technique, future studies need to investigate the effect of peripheral nerve CED on neurological function. Overall, this study provides useful data for future application of this CED technique and a greater understanding of transport dynamics from the peripheral nerve to the spinal cord.

Acknowledgments

This study was supported by a grant from the National Institutes of Health (R21 NS052670). We would like to thank Barbara Beck and Jessica Meloy for their technical assistance in MRI experiments and Dr. Harvey Ramirez for technical assistance in animal surgery. The MRI data were obtained at the Advanced Magnetic Resonance Imaging and Spectroscopy (AMRIS) facility in the McKnight Brain Institute of the University of Florida.

Abbreviations

CED	convection-enhanced delivery
CSF	cerebrospinal fluid
CNS	central nervous system
DCE-MRI	dynamic contrast-enhanced MRI
FOV	field of view
Gd-DTPA	Gadolinium diethylenetriamine penta-acetic acid
GM	gray matter
PBS	phosphate buffered saline
PEEK	polyether-ether-ketone
RF	radio-frequency
TR	time of repetition
TE	time of echo
WM	white matter

REFERENCES

1. Asato F, Butler M, Blomberg H, Gordh T. Variation in rat sciatic nerve anatomy: Implications for a rat model of neuropathic pain. J. Peripher. Nerv. Syst. 2000; 5(1):19–21. [PubMed: 10780679]
2. Behr VC, Weber T, Neuberger T, Vroemen M, Weidner N, Bogdahn U, Haase A, Jakob PM, Faber C. High-resolution MR imaging of the rat spinal cord in vivo in a wide-bore magnet at 17.6 Tesla. Magn. Reson. Mat. Phys. Biol. Med. 2004; 17(3–6):353–358.
3. Bilgen M, Abbe R, Narayana PA. Dynamic contrast-enhanced MRI of experimental spinal cord injury: In vivo serial studies. Magn. Reson. Med. 2001; 45(4):614–622. [PubMed: 11283989]
4. Bobo RH, Laske DW, Akbasak A, Morrison PF, Dedrick RL, Oldfield EH. Convection-enhanced delivery of macromolecules in the brain. Proc. Natl. Acad. Sci. 1994; 91(6):2076–2080. [PubMed: 8134351]
5. Boskamp EB. Improved Surface Coil Imaging in MR - Decoupling of the Excitation and Receiver Coils. Radiology. 1985; 157(2):449–452. [PubMed: 4048454]
6. Chen MY, Lonser RR, Morrison PF, Governale LS, Oldfield EH. Variables affecting convection-enhanced delivery to the striatum: a systematic examination of rate of infusion, cannula size, infusate concentration, and tissue-cannula sealing time. J. Neurosurg. 1999; 90(2):315–320. [PubMed: 9950503]
7. Chen XM, Astary GW, Sepulveda H, Mareci TH, Sarntinoranont M. Quantitative assessment of macromolecular concentration during direct infusion into an agarose hydrogel phantom using contrast-enhanced MRI. Magn. Reson. Imaging. 2008; 26(10):1433–1441. [PubMed: 18583082]
8. Franconi F, Lemaire L, Marescaux L, Jallet P, Le Jeune JJ. In vivo quantitative microimaging of rat spinal cord at 7T. Magn. Reson. Med. 2000; 44(6):893–898. [PubMed: 11108626]
9. Himango WA, Low FN. Fine Structure of a Lateral Recess of Subarachnoid Space in Rat. Anat. Rec. 1971; 171(1):1–20. [PubMed: 5095061]
10. Krauze MT, McKnight TR, Yamashita Y, Bringas J, Noble CO, Saito R, Geletneky K, Forsayeth J, Berger MS, Jackson P, Park JW, Bankiewicz KS. Real-time visualization and characterization of liposomal delivery into the monkey brain by magnetic resonance imaging. Brain Research Protocols. 2005; 16(1–3):20–26. [PubMed: 16181805]
11. Lieberman DM, Laske DW, Morrison PF, Bankiewicz KS, Oldfield EH. Convection-enhanced distribution of large molecules in gray matter during interstitial drug infusion. J. Neurosurg. 1995; 82(6):1021–1029. [PubMed: 7539062]
12. Lonser RR, Gogate N, Morrison PF, Wood JD, Oldfield EH. Direct convective delivery of macromolecules to the spinal cord. J. Neurosurg. 1998; 89(4):616–622. [PubMed: 9761056]
13. Lonser RR, Walbridge S, Garmestani K, Butman JA, Walters HA, Vortmeyer AO, Morrison PF, Brechbiel MW, Oldfield EH. Successful and safe perfusion of the primate brainstem: in vivo magnetic resonance imaging of macromolecular distribution during infusion. J. Neurosurg. 2002; 97(4):905–913. [PubMed: 12405380]
14. Lonser RR, Weil RJ, Morrison PF, Governale LS, Oldfield EH. Direct convective delivery of macromolecules to peripheral nerves. J. Neurosurg. 1998; 89(4):610–615. [PubMed: 9761055]
15. Narayana P, Fenyes D, Zacharopoulos N. In vivo relaxation times of gray matter and white matter in spinal cord. Magn. Reson. Imaging. 1999; 17(4):623–626. [PubMed: 10231189]
16. Pettersson CAV. Drainage of Molecules from Subarachnoid Space to Spinal Nerve Roots and Peripheral-Nerve of the Rat - a Study Based on Evans Blue-Albumin and Lanthanum as Tracers. Acta Neuropathologica. 1993; 86(6):636–644. [PubMed: 7508671]
17. Ratliff JK, Oldfield EH. Convection-enhanced delivery in intact and lesioned peripheral nerve. J. Neurosurg. 2001; 95(6):1001–1011. [PubMed: 11765815]
18. Stopa B, Rybarska J, Drozd A, Konieczny L, Krol M, Lisowski M, Piekarska B, Roterman I, Spolnik P, Zemanek G. Albumin binds self-assembling dyes as specific polymolecular ligands. Int. J. Biol. Macromol. 2006; 40(1):1–8. [PubMed: 16769109]
19. Tao L, Nicholson C. Diffusion of albumins in rat cortical slices and relevance to volume transmission. Neurosci. 1996; 75(3):839–847.
20. van den Berg MP, Romeijn SG, Verhoef JC, Merkus FW. Serial cerebrospinal fluid sampling in a rat model to study drug uptake from the nasal cavity. J. Neurosci. Meth. 2002; 116:99–107.

21. Williams, PL.; Warwick, R., editors. Gray's anatomy. 36th ed.. Philadelphia: W.B. Saunders; 1980. 1578 p.

22. Wood JD, Lonser RR, Gogate N, Morrison PF, Oldfield EH. Convective delivery of macromolecules into the naive and traumatized spinal cords of rats. J. Neurosurg. 1999; 90(1): 115–120. [PubMed: 10413135]

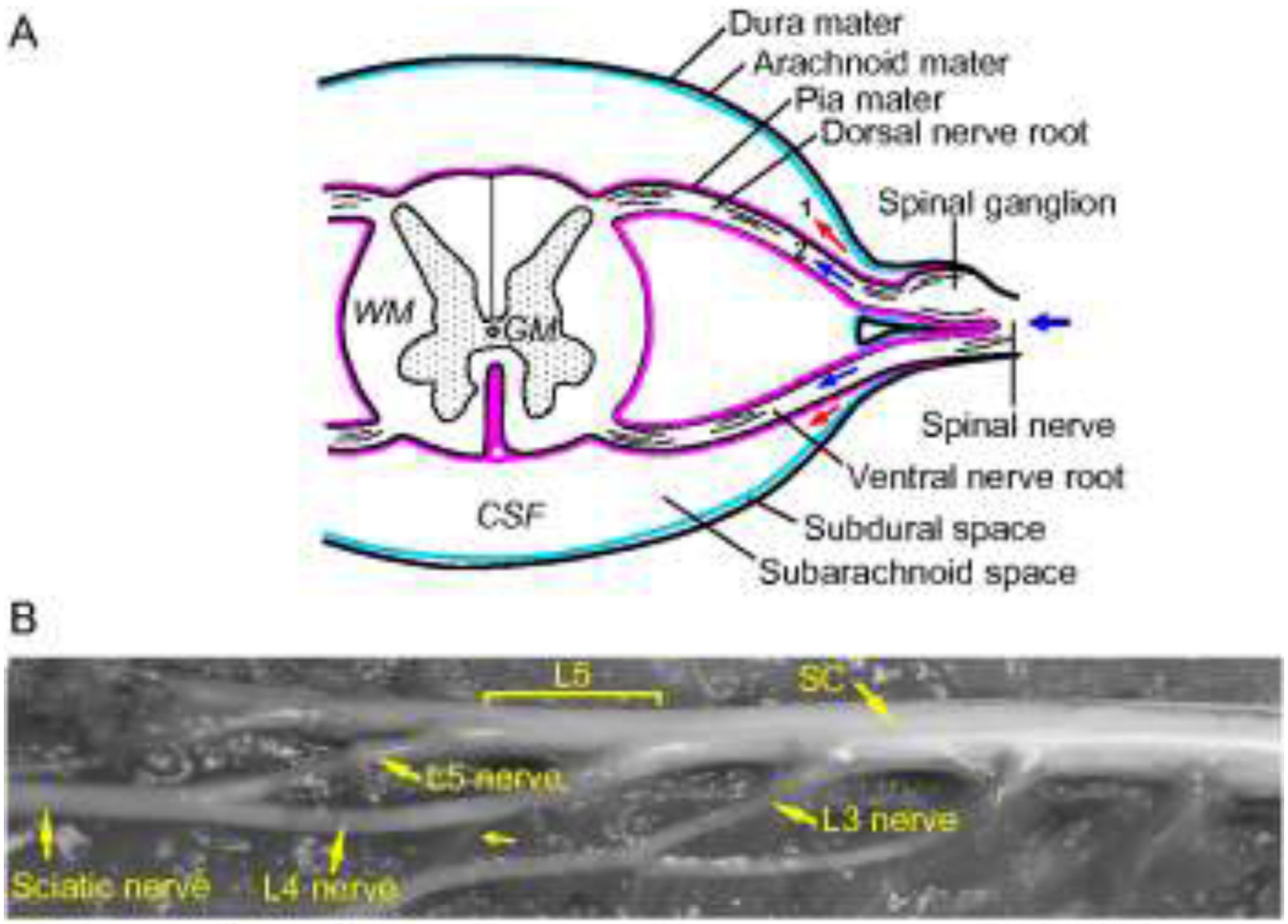

Figure 1.

(**A**) Schematic of the anatomy of the spinal cord region (GW: gray matter; WM: white matter; CSF: cerebrospinal fluid). Arrows indicate the potential transport pathways for peripheral nerve CED: (Path 1) into the CSF; (Path 2) along the nerve root. Background picture was adapted from [21]. (**B**) External anatomy of the rat sciatic nerve, spinal cord and other connected spinal nerves. A single sciatic nerve divides into two major branches, spinal nerves L4 and L5, which enter the spinal cord region at vertebral levels L4 and L5, respectively. A thin connection (small arrow) between spinal nerves L4 and L3 is also present (SC: spinal cord).

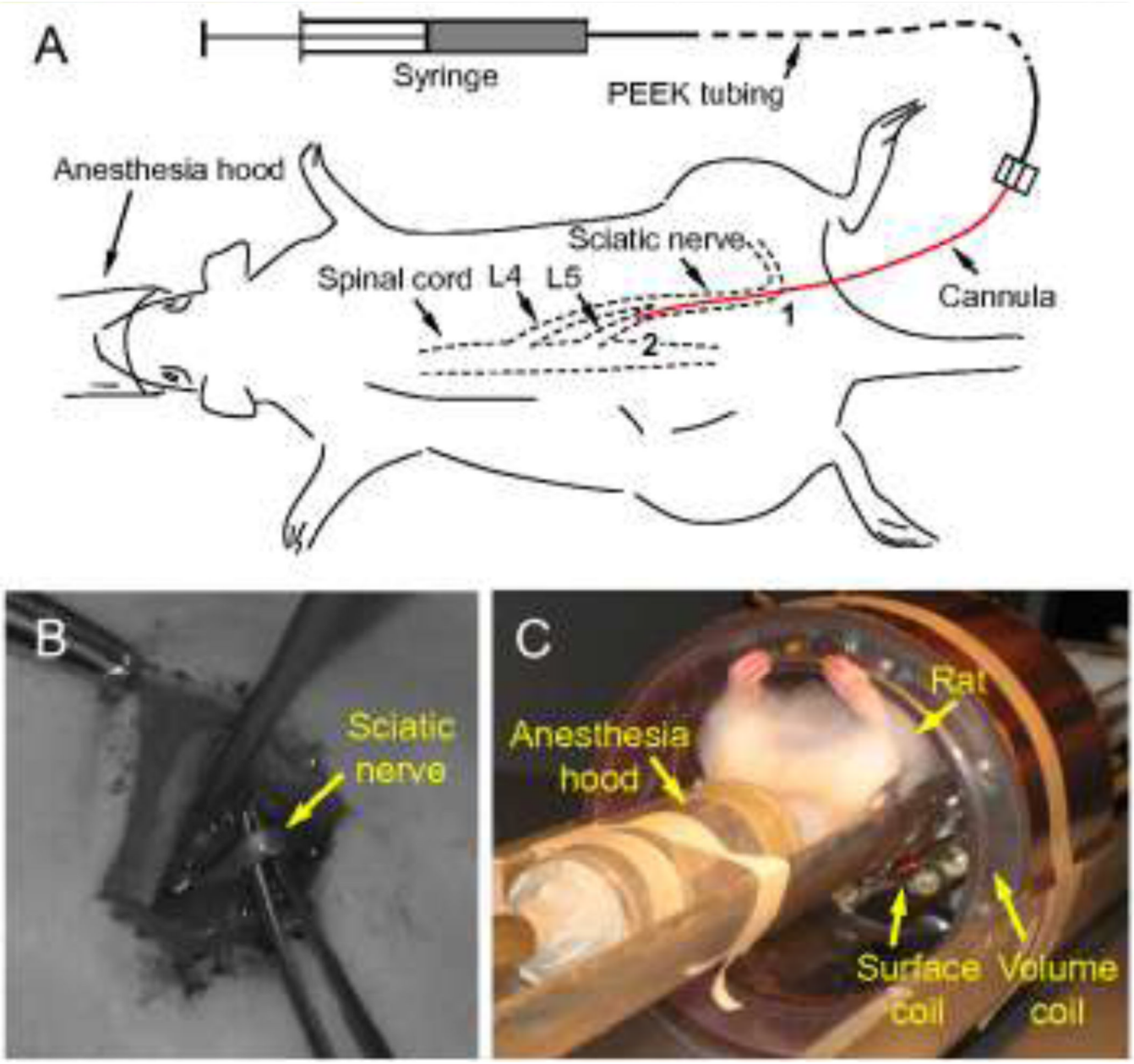

Figure 2.

(**A**) Schematic of sciatic nerve infusion. Point 1 is the insertion point where the infusion cannula was introduced into the sciatic nerve. Point 2 is the location of the cannula tip. Cannula length from points 1 to 2 is defined as the insertion depth. (**B**) The isolated rat sciatic nerve. (**C**) The RF dual coil system with an anesthetized rat used to collect MRI data.

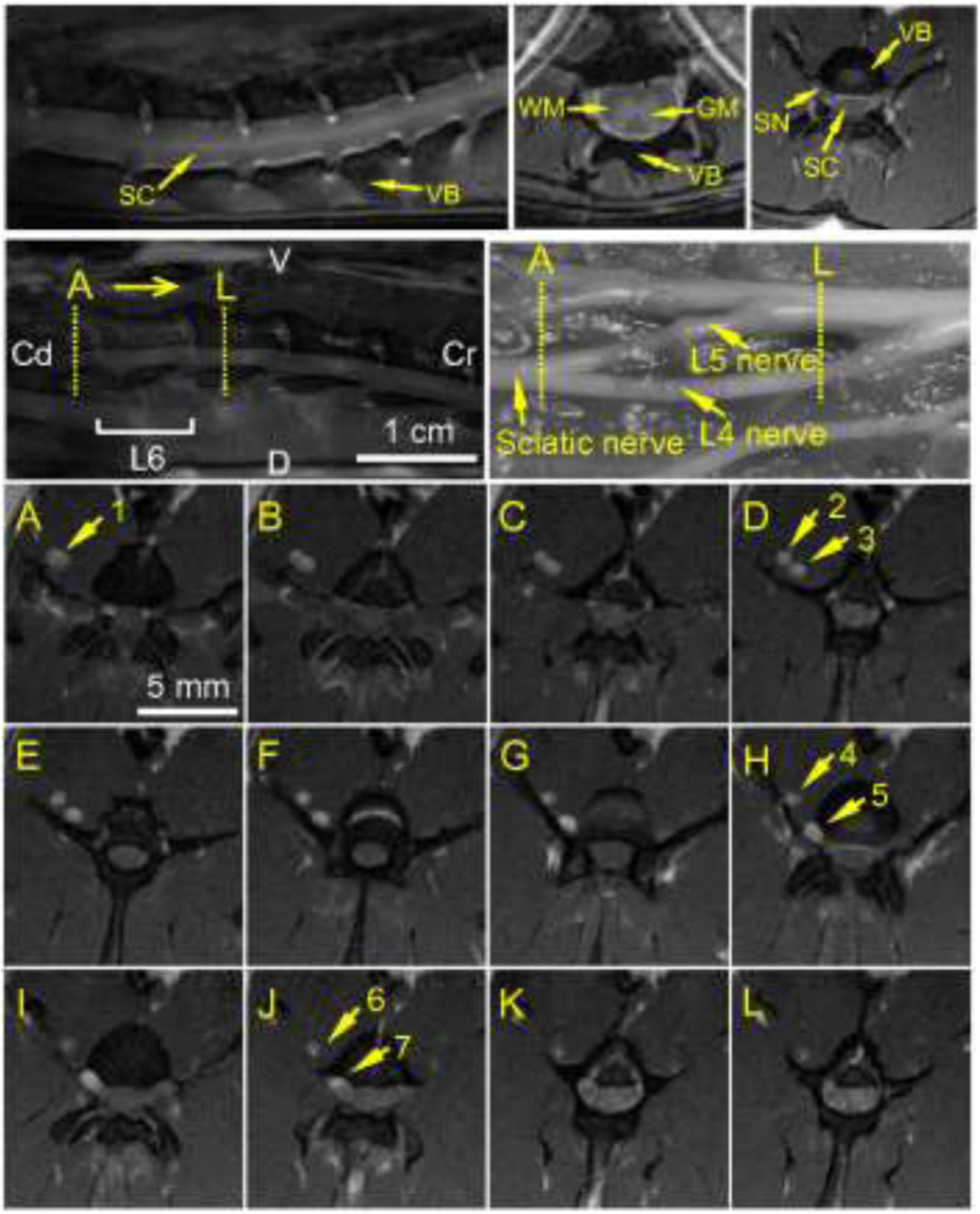

Figure 3.

Typical MR images of the rat spinal cord with fat suppression: (Left) sagittal scan; (Middle) transverse scan at a high vertebral level L1; (Right) transverse scan at a low vertebral level L6 (VB: vertebral bone; SC: spinal cord; SN: spinal nerve). The overlap on the left and right sides is a folding artifact. MRI acquisition resolution: 0.16 mm × 0.16 mm × 1 mm per voxel; reconstructed image resolution: 0.08 mm × 0.08 mm × 1 mm per voxel.

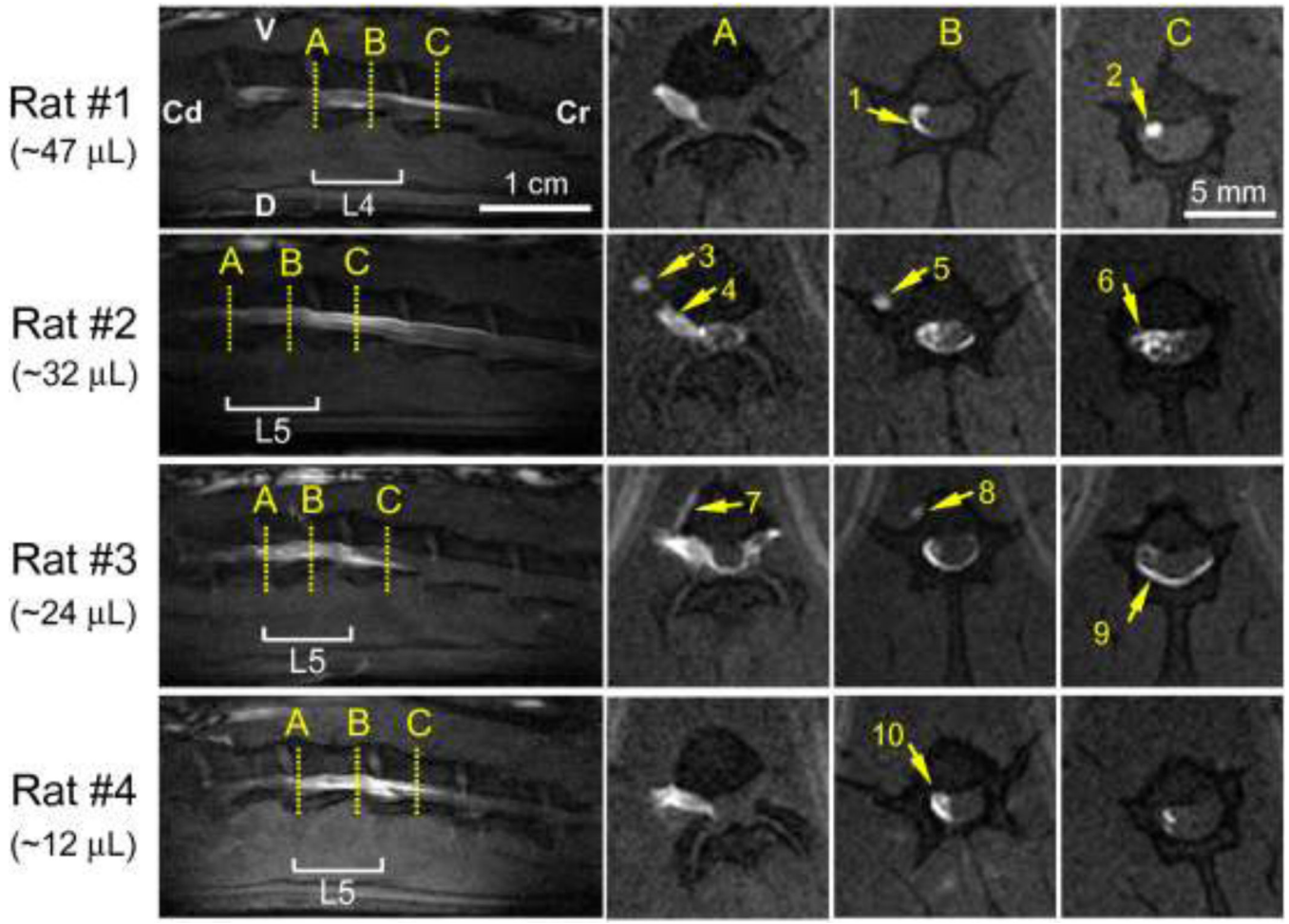

Figure 4.

Distribution of Gd-DTPA within the sciatic nerve at the end of CED (~70 µL infusion). (Top) Sagittal scan of the spinal cord region and anatomical view of the vertebral levels where MR images were acquired (V: ventral; D: dorsal; Cr: cranial; Cd: caudal). (A–L) Transverse MR scans covering vertebral levels L6-L5. Scans are ordered in the caudal-cranial direction with MR slice thickness = 1 mm. Arrows point to enhanced regions: (1) in the sciatic nerve; (2, 4, & 6) in the L4 nerve; (3, 5, & 7) in the L5 nerve. MR images are from a preliminary infusion study using a short cannula insertion depth of ~1 cm. MRI acquisition resolution: 0.2 mm × 0.2 mm × 1 mm per voxel; reconstructed image resolution: 0.1 mm × 0.1 mm × 1 mm per voxel.

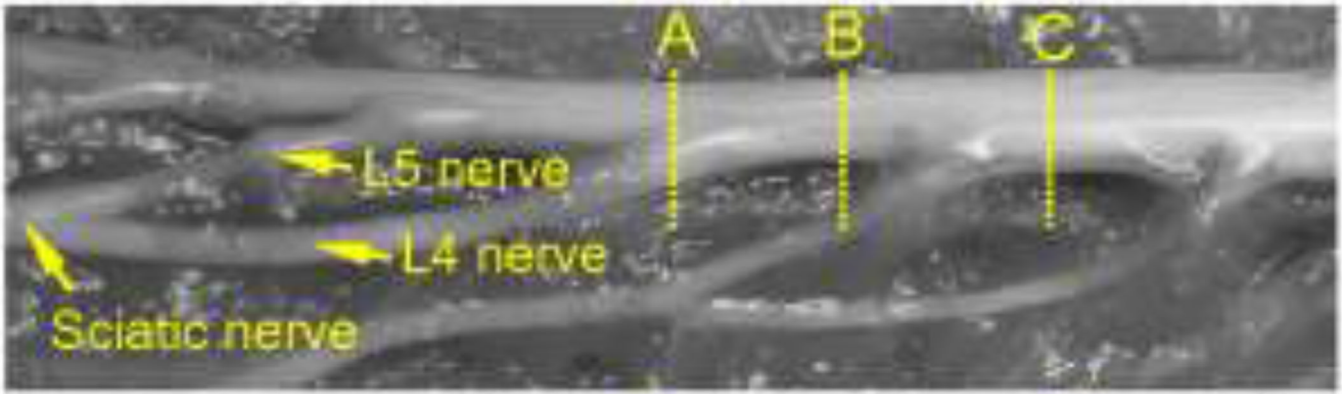

Figure 5.
Tracer distributions of Gd-DTPA-albumin in the spinal cord region after sciatic nerve CED into different rats. (Left column) Sagittal scans of the spinal cord region (V: ventral; D: dorsal; Cr: cranial; Cd: caudal). (Columns A–C) Transverse scans showing a caudal view at positions A–C. Arrows show various tissue distributions: (1, 6, & 9) in the CSF; (2) in nerve roots; (3 & 5) along the L4 nerve; (4) through the L5 nerve; (7 & 8) leakage into the surrounding tissue; (10) in the CSF and nerve roots. Rats #1–4 share a similar cannula insertion depth of 3.5–4 cm. MRI acquisition resolution: 0.2 mm × 0.2 mm × 1 mm per voxel; reconstructed image resolution: 0.1 mm × 0.1 mm × 1 mm per voxel.

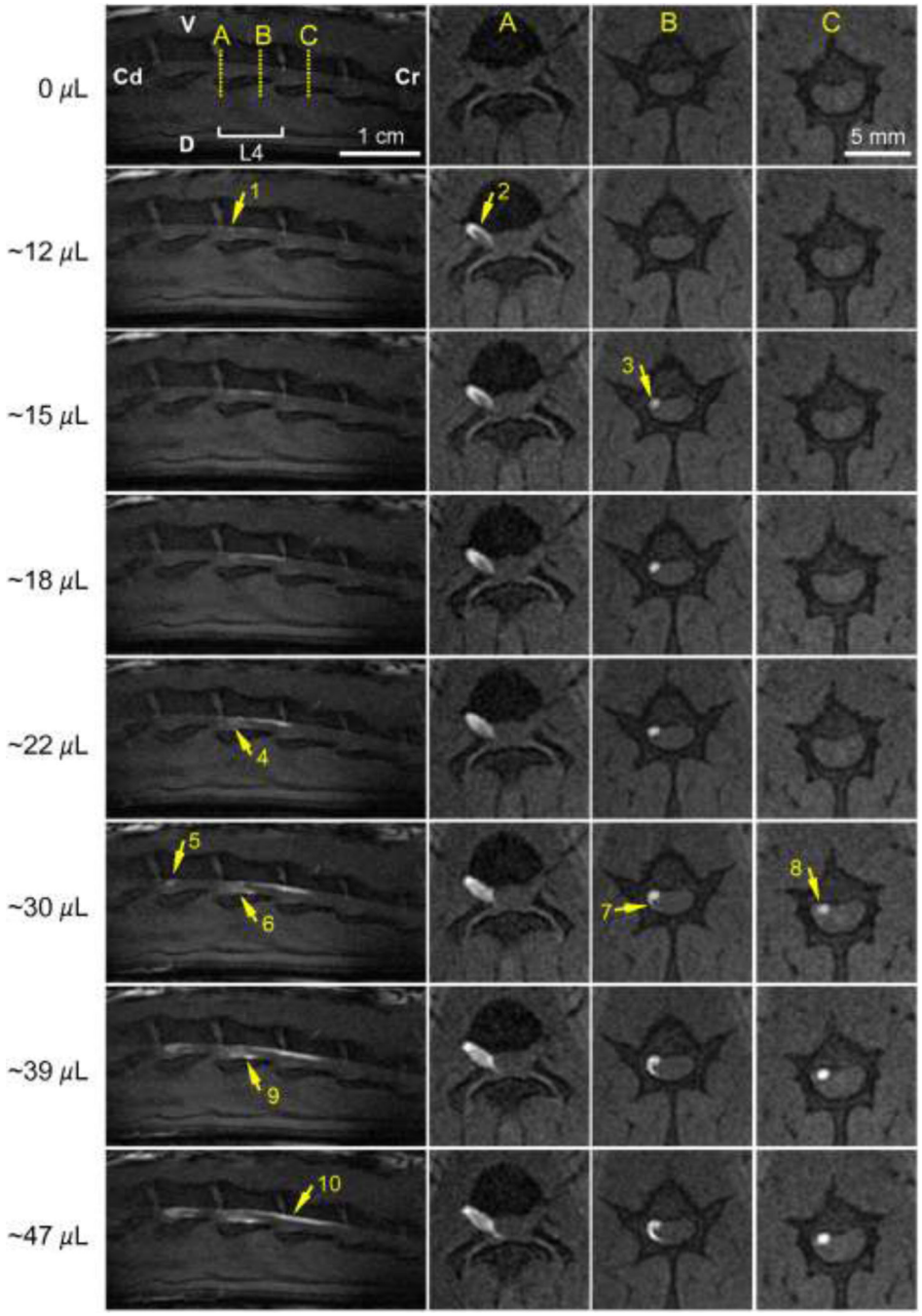

Figure 6.

Consecutive sagittal and transverse scans of the spinal cord region during sciatic nerve CED of Gd-DTPA-albumin (infusion rate=0.3 μL/min). (Top) Anatomical view of the vertebral levels scanned. (Left column) Sagittal scans covering vertebral levels from L2 to L5 (V: ventral; D: dorsal; Cr: cranial; Cd: caudal). (Columns A–C) Transverse scans showing a caudal view at positions A–C. Arrows show tracer tracking into the spinal cord region: (1 & 2) from the L4 spinal nerve; (3, 8 & 10) up along a nerve root; (4, 6, 7& 9) into the CSF; (5) from the L5 spinal nerve. MR images are for rat #1. MRI acquisition resolution: 0.2 mm × 0.2 mm × 1 mm per voxel; reconstructed image resolution 0.1 mm × 0.1 mm × 1 mm per voxel.

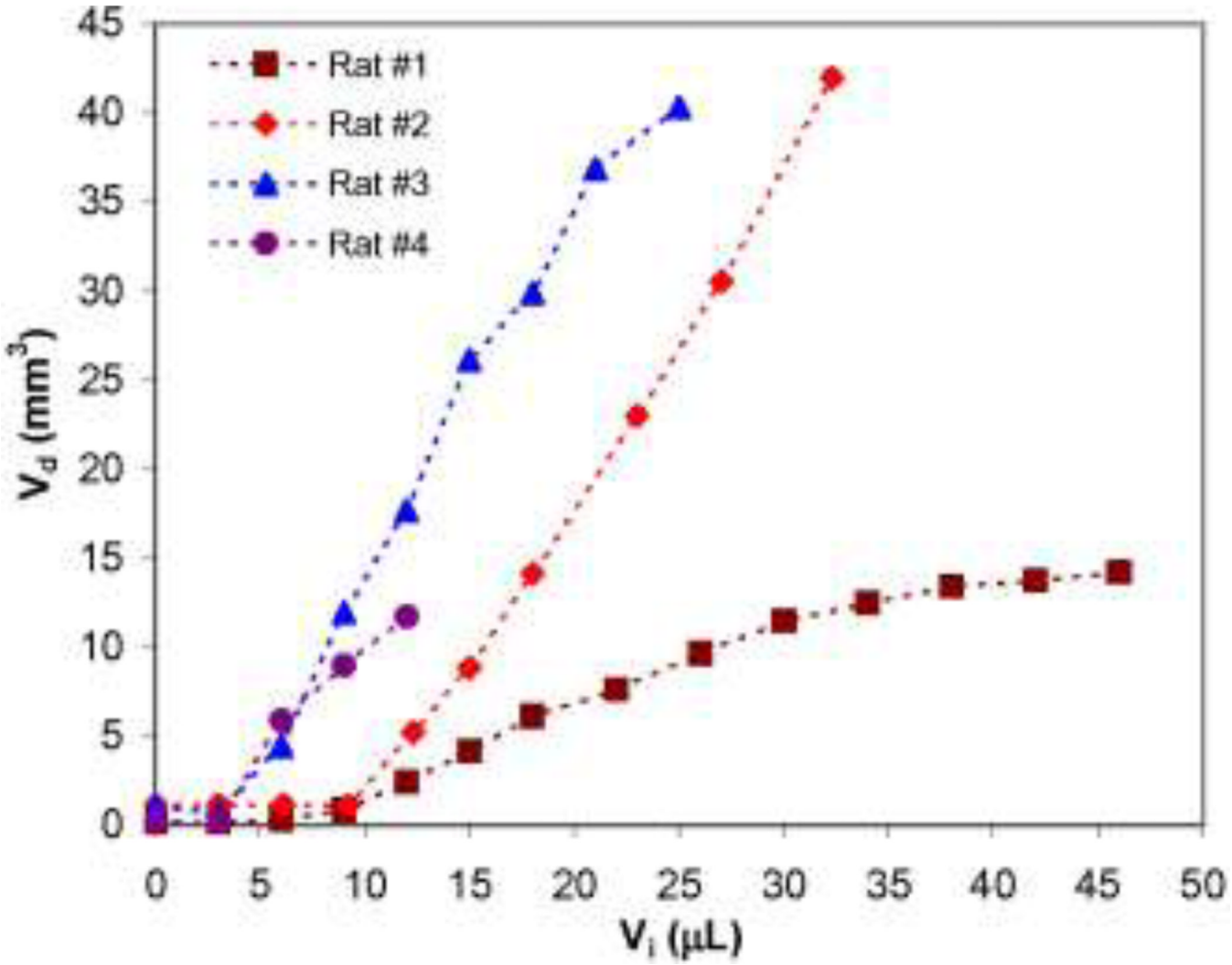

Figure 7.
Tissue distribution volumes (Vd) within the spinal cord region with increasing tracer infusion volumes (Vi) for a constant infusion rate of 0.3 µL/min. Note that Vd did not include tracer distribution in peripheral nerve and the initial distribution delay was due to tracer being confined in the peripheral nerve while still outside the spinal cord region.

Table 1

Summary of peripheral nerve CED infusion parameters and Gd-DTPA-albumin tracer distribution results for the spinal cord region.

Rat	Volume infused (μL)	L4/L5 entry	CSF distribution	Nerve root distribution	Axial distribution length* (mm)
1	47	L4	Yes	Yes	22
2	32	L5	Yes	Yes	25
3	24	L5	Yes	Yes	15
4	12	L5	Yes	Yes	14

* approximated from sagittal scans.